THE ASTROPHYSICAL JOURNAL, 466:938–945, 1996 August 1

THE MORPHOLOGY OF YOUNG NEUTRON STARS: PSR B1823−13, ITS COMPACT NEBULA, AND ITS INTERSTELLAR NEIGHBORHOOD

JOHN P. FINLEY,[1] RADHIKA SRINIVASAN,[2] AND SANGWOOK PARK[3]
Department of Physics, Purdue University, 1396 Physics Building, West Lafayette, IN 47907
Received 1995 November 29; accepted 1996 February 14

ABSTRACT

The young 21,000 yr old neutron star PSR B1823−13 was imaged by both the PSPC and HRI aboard *ROSAT* during 1993 and 1994. The data reveal that the morphology of PSR B1823−13 is similar to other neutron stars of a similar age. The pointlike neutron star component is found embedded in a compact nebula of radius $\sim 20''$ and surrounded by a low surface brightness diffuse emission region of extent $\sim 4'$–$5'$. The diffuse extended component is consistent with the size expected for an associated remnant given the observed size of the compact nebula. Alternatively, the extended component may be a pulsar wind nebula and, if so, PSR B1823−13 cannot be a high-velocity neutron star unless it is embedded in an unusually rarefied region of the interstellar medium. Limits on the surface temperature of the bare neutron star are derived and compared with current models.

Subject headings: pulsars: individual (PSR B1823−13) — stars: neutron — supernova remnants — X-rays: stars

1. INTRODUCTION

Studies of young neutron stars have direct impact on some poorly understood areas of pulsar astrophysics: the mechanism whereby pulsars shed their spin-down energy, the electrodynamics of the pulsar magnetosphere, the state of matter above nuclear density, pulsar birth velocities, and supernova remnant (SNR) evolution to name but a few. Progress has been slow due to the dearth of young neutron stars known in our Galaxy. However, recent high-frequency radio surveys have increased the detected number of young[4] (i.e., $\leq 10^5$ yr.) neutron stars dramatically (Clifton et al. 1992; Johnston et al. 1992; Clifton & Lyne 1986), and the present pulsar catalog contains some 708 pulsars of which 21 are, by our definition, young (Taylor, Manchester, & Lyne 1995). This increased sample coupled with advances in radio imaging, particularly at low frequencies, has revealed that perhaps as many as 15 of these young pulsars are in association with SNRs (see Frail, Goss, & Whiteoak 1994a for a recent discussion). The systematic study of these pulsar/SNR associations indicates, as first pointed out by Caraveo (1993), that the population of pulsars may have much higher birth velocities than previous estimates based upon statistical analysis of their spatial distribution (Gunn & Ostriker 1970) and proper motion surveys (Cordes 1986). The association of a pulsar and SNR also has the distinct advantage of providing a cross check on the age and distance to the system and offers a unique probe of the ambient gas filling the interstellar medium (ISM) (Shull, Fesen, & Saken 1989).

Progress in pulsar astrophysics has been aided by observations at very short wavelengths as well. Recent space-based missions have uncovered over 10 X-ray emitting isolated neutron stars (see Ögelman 1994 for a review), most of which are young, and a handful of γ-ray pulsars (Thompson et al. 1994), all of which are young. At the highest observable energies of a few hundred GeV, the domain of ground-based atmospheric Cerenkov γ-ray astronomy, young pulsars account for more than half of the catalog of sources (Vacanti et al. 1991; Kifune et al. 1995). Given that most of the observed flux emerges at very short wavelengths, these high-energy bands are providing crucial clues to the energetics of young pulsars.

During the mid 1980s a high-frequency survey of the Galactic plane was carried out at Jodrell Bank with the aim of discovering young and distant pulsars (Clifton et al. 1992). The survey of Clifton et al. (1992) discovered some 40 new pulsars of median age 8×10^5 yr, three of which, PSRs B1727−30, B1800−21, and B1823−13, were remarkable for their very young age of $\sim 2 \times 10^4$ yr (Clifton & Lyne 1986). If these pulsars were born in a supernova event and the lifetime of Galactic SNRs is $\geq 20{,}000$ yr, it would be reasonable to expect a pulsar/SNR association for each. The reality, however, often diverges from expectation. Braun, Goss, & Lyne (1989) imaged the fields of PSRs B1727−30, B1800−21, and B1823−13 using the VLA in the C and C/D configuration in an attempt to detect the presence of the putative SNRs. Their observations failed to detect any SNR or pulsar-powered nebula associated with any of the candidates, and they called into question currently accepted ideas regarding neutron star formation and SNR observable lifetimes (Braun et al. 1989). However, subsequent imaging of the field containing PSR B1800−21 at high resolution has led to a suggested association between the pulsar and the molecular cloud complex W30 (Odegard 1986; Kassim & Weiler 1990; Frail, Kassim, & Weiler 1994b)—an association further supported by deep X-ray imaging observations utilizing *ROSAT* (Finley & Ögelman 1994). The PSR B1800−21/W30 association is not without its problems though and requires either that the pulsar have a very large transverse velocity, as recent work on birth velocities may support (Caraveo 1993; Frail, Goss & Whiteoak 1994a), or that the supernova occurred in a highly nonuniform ISM (Odegard 1986; Finley & Ögelman 1994). The SNRs associated with both PSR B1727−30 and PSR B1823−13 as yet remain undetected.

[1] finley@purds1.physics.purdue.edu.
[2] radhika@purds1.physics.purdue.edu.
[3] parksan@purds1.physics.purdue.edu.
[4] We arbitrarily choose to define young neutron stars as those having timing ages of $\leq 10^5$ yr.

TABLE 1

THE PARAMETERS OF PSR B1823−13

Period (ms)	$\dot{P}$ (10^{-15} s s^{-1})	log τ (yr)	log $\dot{E}$ (ergs s^{-1})	DM (pc cm^{-3})	Distance (kpc)
101.45.....	74.945	4.33	36.45	231	4.12

In this article we report on deep X-ray observations of the young neutron star PSR B1823−13 utilizing both the position sensitive proportional counter (PSPC) and the high resolution imager (HRI) carried aboard the space-based observatory *ROSAT*. The rotational parameters of PSR B1823−13 ($P = 101$ ms, $\dot{P} \cong 75 \times 10^{-15}$ s s^{-1}) indicate a dynamic age of ~21,000 yr, and a spindown energy loss rate of $\sim 3 \times 10^{36}$ ergs s^{-1}, among the youngest and most energetic pulsars in the current catalog (Taylor et al. 1995) and very similar to the Vela pulsar. The aim of the observations was the detection of the pulsar as a source of X-ray emission, characterization of both the emission spectrum and morphology of the system, and to search for evidence of the SNR which would be expected to be associated with such a young neutron star. In § 2 we will describe the observations while in § 3 results of the analysis are given. A discussion of the implications of the observations can be found in § 4 and, finally, a short summary is given in § 5.

2. OBSERVATIONS

PSR B1823−13 was observed as part of a *ROSAT* program intended to detect young isolated radio pulsars in the soft X-ray band. Detailed descriptions of the satellite, X-ray mirrors, and detectors can be found in Pfeffermann et al. (1986). Briefly, both the PSPC and the HRI are sensitive in the soft X-ray band 0.1–2.4 keV. The PSPC has an on-axis energy response of $E/\Delta E \sim 2.3$ at 0.93 keV and an effective spatial resolution of ~25″. The HRI has no effective energy response but an effective spatial resolution on axis of ~1.7″ full width at half-maximum (FWHM). The parameters of PSR B1823−13 are listed in Table 1.

The PSPC data were acquired in two observing sessions; 1992 October 12 and 1993 March 22. The two separate data sets were combined to yield an effective exposure time on-axis of 14,706 s. The follow-up HRI observations, intended to give detailed morphological information, were

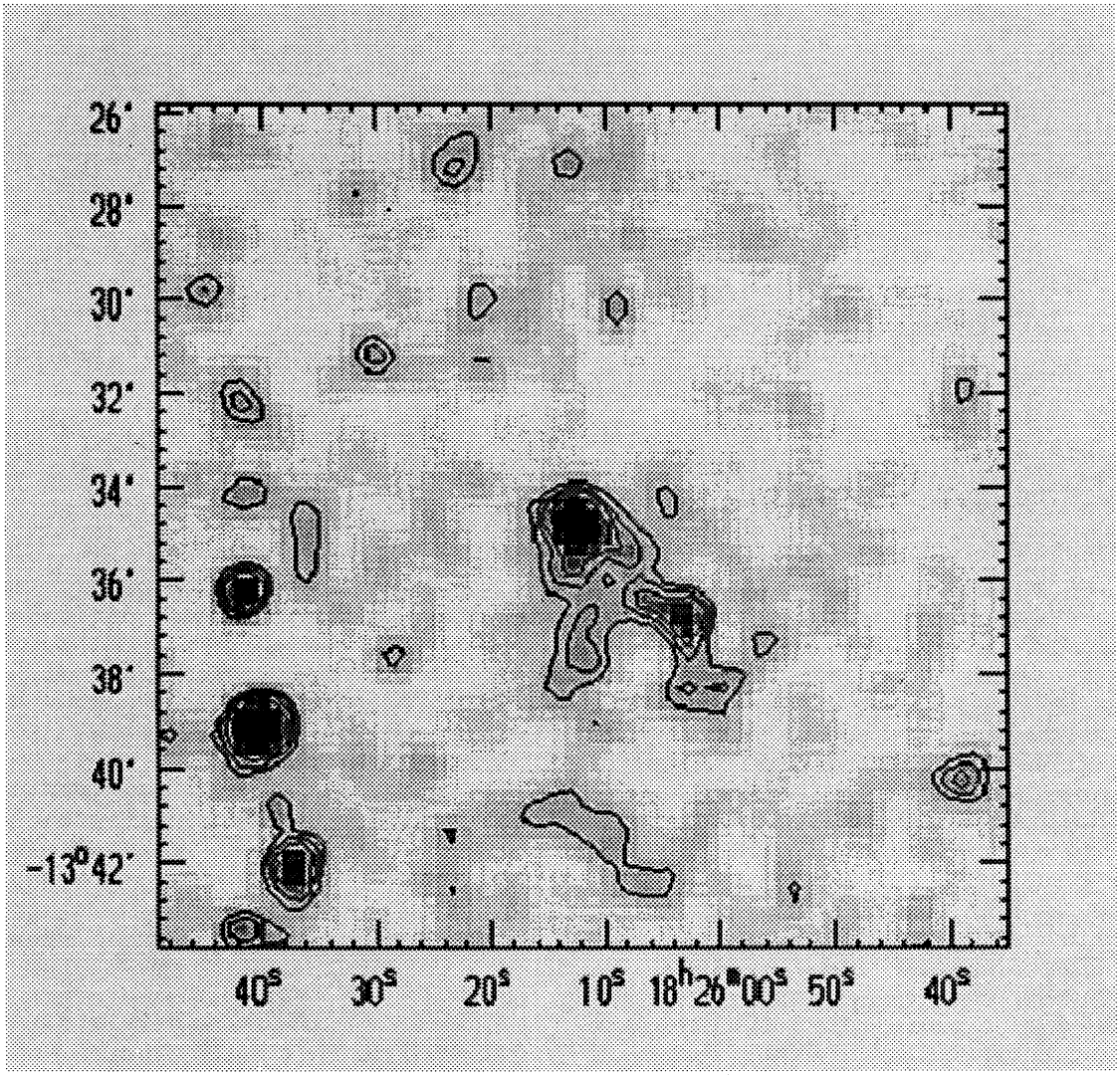

FIG. 1.—A gray scale of the central region of the PSPC image after smoothing with a 1.′3 FWHM Gaussian. The contours are 35%, 40%, 45%, and 55% of the peak value in the image. A low surface brightness diffuse emission region is observed surrounding PSR B1823−13 which is the center of the field. The point source at position $\alpha = 18^h26^m40^s$ and $\delta = -13°39'$ is the O6 star HD 169727 (see text). In the image north is up and east is to the left.

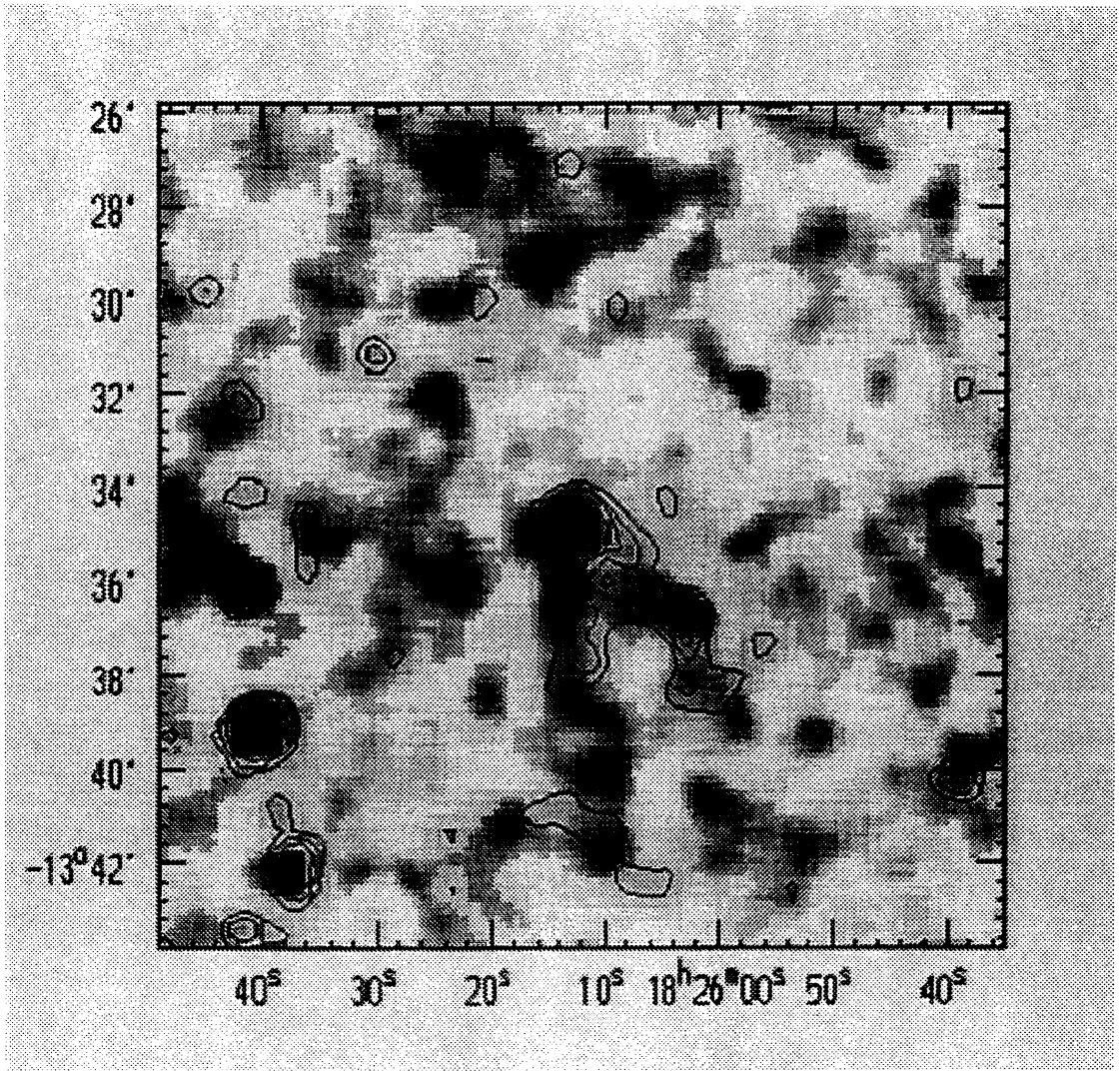

FIG. 2.—A gray scale of the central region of the HRI image after smoothing with a 1.'3 FWHM Gaussian. The contours are from the PSPC image (see Fig. 1). The noisy appearance of the image compared to the PSPC is a result of the lower surface brightness sensitivity of the HRI compared with the PSPC. The horizontal line at the top of the image and the small vertical line at the lower right were aids in the alignment.

acquired on 1994 September 16. The effective on-axis exposure with the HRI at the focus of the telescope was 32,305 s. The central region of the PSPC image, after application of a 1.'3 FWHM Gaussian smoothing algorithm, is displayed in Figure 1. PSR B1823−13 is detected (Finley & Ögelman 1993) and, as inspection of Figure 1 reveals, appears embedded in an ∼4′ low surface brightness diffuse emission region. The source position (J2000) as determined from the PSPC data is $\alpha = 18^h26^m13^s$, $\delta = -13°34'50''$ which is in excellent agreement with the established radio timing position (Taylor et al. 1995). The background-subtracted, vignetting-corrected PSPC counting rate in a ring of radius 5′ centered on the position of PSR B1823−13 is 8.7 ± 0.8 counts ks^{-1}. This counting rate, however, includes the contribution from the diffuse emission surrounding PSR B1823−13 and does not represent the counting rate from the bare neutron star. We will address the isue of the pulsar countiong rate in § 3. In addition to PSR B1823−13 several other point sources are observed south and east of the pulsar (see Fig. 1). One of those additional sources is identified as the O6 star HD 169727 at $\alpha = 18^h26^m40^s$, $\delta = -13°39'7''$. Its presence within the field of view of both the PSPC and the HRI is useful for checking the astrometric solution and provides a check of the attitude reconstruction. The pointlike nature of the radial profile of HD 169727 at its position within the detector assures us that the extended emission observed surrounding PSR B1823−13 is not an artifact of imprecision in the attitude reconstruction. The central region of the HRI image, after application of a 1.'3 FWHM Gaussian smoothing algorithm, is displayed in Figure 2 with the contours from the PSPC superposed. The background-subtracted, vignetting-corrected counting rate of PSR B1823−13, extracted from the region of the sky coincident with that utilized in the PSPC is 8.6 ± 1.1 counts ks^{-1}. The "noisy" appearance of the image in Figure 2 is due to the lower signal-to-noise ratio of the HRI data. In general, the extended emission features observed in the PSPC data are present, albeit somewhat weaker due to the low surface brightness sensitivity of the HRI, in Figure 2. The agreement of the source position as derived from the HRI data is, again, in excellent agreement with the radio timing position of Taylor et al. (1995).

3. RESULTS

To ascertain the small-scale morphology of the system we utilized the HRI data and extracted the photons from a 150″ ring centered on the pulsar position. The background level was determined by sampling several regions surrounding the source region and averaging. The radial profile of the source + background counts was then fitted to a model of the form

$$N(r) = N_{\rm PS} \times {\rm PSF}(r) + \frac{N_{\rm CN}}{2\pi r_{\rm CN}^2}\, e^{-r/r_{\rm CN}} \times {\rm PSF}(r) + N_{\rm EX} + N_B\,,$$

where the free parameters are $N_{\rm PS}$, the number of point source photons, $N_{\rm CN}$, the number of compact nebular photons, and $r_{\rm CN}$, the radius of the compact nebular component. The function PSF(r) is the normalized point spread function at the appropriate off-axis angle, $N_{\rm EX}$ are the counts per square arcmin due to the extended component observed in Figure 1, and N_B is the average background level per square arcmin. The extended counts are constrained by the relation $N_{\rm EX} = N - N_{\rm PS} - N_{\rm CN} - N_B$, where N is the integrated number of observed counts within our extraction radius. The model yielded best-fitting values of $N_{\rm PS} = 5$ counts, $N_{\rm CN} = 60$ counts, and $r_{\rm CN} = 19''$. This best-fitting model constrained the extended component to be $N_{\rm EX} = 212$ counts. The radial profile and the best-fitting model are displayed in Figure 3. We attempted to fit the data in Figure 3 with a point source plus an extended component only but no satisfactory fit could be found. We checked for consistency of the best-fit model parameters derived from the HRI by comparing the results with the observed PSPC radial distribution. The PSPC radial distribution was found consistent with the model derived from the HRI data. The scarcity of counts from any of the individual components made it difficult to constrain the lower limit of the best-fit values given above. We therefore derived 90% confidence level (CL) upper limits for each of the individual components following the procedure of Lampton, Margon, & Bowyer (1976). The 90% CL upper limit on the point source component yielded $N_{\rm PS} \leq 23$ counts in the HRI and a corresponding 90% CL upper limit of $N_{\rm PS} \leq 32$ counts in the PSPC. The corresponding compact nebular components were $N_{\rm CN} \leq 28$ and $N_{\rm CN} \leq 34$ counts while the extended component totals were $N_{\rm EX} \leq 226$ counts and $N_{\rm EX} \leq 62$ counts for the HRI and PSPC, respectively. The linear scale of the compact nebula, based on the HRI data, was constrained to be less than 30″ and was held fixed at the best-fitting value of 19″ to derive the 90% CL upper limits. The PSPC radial profile indicates a maximum linear scale size of the extended component of 4′.

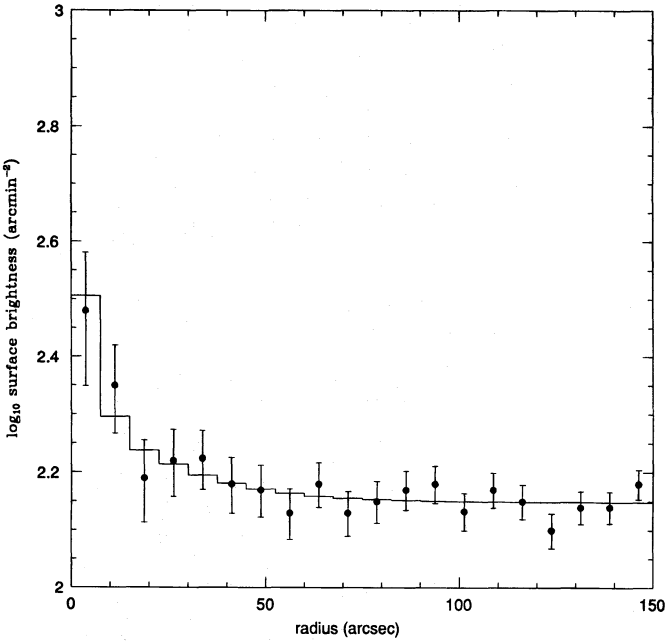

FIG. 3.—The radial surface brightness distribution (counts arcmin^{-2}) from the HRI image within a 150″ circle centered on PSR B1823−13. The histogram is the best-fitting model incorporating a point source, compact nebula, and extended component (see discussion in the text).

The spectral properties of the system were modeled based upon the 90% CL upper limits derived from the radial distributions. A source model was chosen, propagated, and absorbed in the ISM, folded through the detector response and the resulting counting rate was compared with the derived upper limits. The presence of the O6 star HD 169727 within the detector field of view aided in constraining the equivalent neutral hydrogen column density along the line of sight toward PSR B1823−13. The measured extinction toward HD 169727 is $E(B-V)_{\rm O} = 0.79$ mag (Garmany & Vacca 1991) which, with the intrinsic $B-V$ of −0.32 for a zero-age main-sequence star of spectral class O6, yields an extinction of $E(B-V) = 1.11$ mag. This extinction corresponds to a neutral hydrogen column density of $N_{\rm H} = 6.5 \times 10^{21}$ cm^{-2} upon applying the relation between total hydrogen and extinction of Bohlin, Savage, & Drake[5] (1978). The distance to HD 169727 derived from the distance modulus and the observed $m_v = 9.28$ (Garmany & Vacca 1991) is 2.9 kpc. Given that the dispersion measure derived distance to PSR B1823−13 is 4.2 kpc we adopted a lower limit of $N_{\rm H} > 8 \times 10^{21}$ cm^{-2} for the interstellar neutral hydrogen column density along the line of sight toward the pulsar. Under the assumption that there are no additional contributions to the dispersion measure due to H II regions along the line of sight toward PSR B1823−13 the measured DM implies an average $N_{\rm H}$ of 2×10^{22} m^{-2}. To allow for uncertainty in the average electron density in the Galaxy and the distance to PSR B1823−13 of 3 kpc $\leq d \leq$ 5 kpc (Taylor, Manchester, & Lyne 1993), we adopt as an upper limit to the $N_{\rm H}$ twice the value inferred from the DM, which is 4×10^{22} cm^{-2}. Thus the spectral modeling was carried out with the $N_{\rm H}$ constrained to the range 8×10^{21} cm$^{-2} \leq N_{\rm H} \leq 4 \times 10^{22}$ cm^{-2}.

The 32 PSPC point source photons (90% CL upper limit) were assumed to arise as a result of the cooling of the neutron star and originate from the stellar surface with a blackbody spectrum. With the distance fixed at 4 kpc and for stellar radii in the range 8–16 km we derived the blackbody temperature consistent with the observed counting rate to be $T_\infty = 2.4 \times 10^6$ K (90% CL upper limit) with an

[5] $\left(\frac{\langle N({\rm H\,I} + {\rm H}_2)\rangle}{\langle E(B-V)\rangle}\right) = 5.8 \times 10^{21}$ cm^{-2} mag^{-1}.

equivalent hydrogen column density of 4×10^{22} cm^{-2}. The correspondong unabsorbed blackbody flux in the 0.5–2.4 keV band is $F_X \leq 6 \times 10^{-12}$ ergs cm^{-2} s^{-1} or, assuming a distance of 4 kpc, a bolometric source luminosity of $L_X \leq 1.6 \times 10^{34}$ ergs s^{-1}. If the point source photons are a result of electromagnetic processes in the outer magnetosphere a nonthermal description is the appropriate model choice. For a Crab-like spectrum (i.e., power-law distribution with energy index $\alpha = -1.0$) the unabsorbed 0.5–2.4 keV flux is $F_X \leq 2.2 \times 10^{-12}$ ergs cm^{-2} s^{-1} corresponding to a source luminosity of $L_X \leq 3.8 \times 10^{33}$ ergs s^{-1}. The compact nebular counts were modeled assuming a nonthermal power-law spectra of energy index $\alpha = -1.0$, similar to the spectrum observed from the Vela pulsar's compact nebula (Ögelman, Finley, & Zimmermann 1993). The 90% CL upper limit unabsorbed flux which describes the data is $F_X \leq 2.4 \times 10^{-12}$ ergs cm^{-2} s^{-1} corresponding to a source luminosity of $L_X \leq 4 \times 10^{33}$ ergs s^{-1}. Compared to the spin-down luminosity of the neutron star ($\dot{E} = I\omega\dot{\omega}$) this luminosity represents at most $\sim$0.15% of the available energy and is consistent with observations of the Vela pulsar ($L_X/\dot{E} \sim 0.03\%$) (Ögelman et al. 1993), PSR B1951+32 ($L_X/\dot{E} \sim 0.2\%$) (Safi-Harb, Ögelman, & Finley 1995), and PSR B1509−58 ($L_X/\dot{E} \sim 0.2\%$) (Greiveldinger et al. 1995). It is possible to fit the data to a compact nebular component and extended component only (i.e., no point source) within 90% CL limits but this description relegates essentially all the photons (>90%) to the compact nebular component which we view as highly unlikely given the large physical size this would imply for the compact nebula. The extended component, which was constrained by the point source plus compact nebular counts as described earlier, was alternatively modeled with both a thermal and nonthermal spectrum. In the case of the nonthermal description a Crab-like spectrum ($\alpha = -1.0$) yields an unabsorbed flux limit of $F_X \leq 5 \times 10^{-12}$ ergs cm^{-2} s^{-1} while a thermal plasma Raymond-Smith model with solar abundance leads to an unabsorbed flux limit of $F_X \leq 1 \times 10^{-11}$ ergs cm^{-2} s^{-1} for a plasma temperature of 10^7 K. A. Raymond-Smith plasma model with plasma temperature of 10^6 K would imply a flux limit some three orders of magnitude higher and an unreasonably large source luminosity and we thus conclude that the data, if they are to be described by a thermal model, naturally favor very high source temperatures. A summary of the modeling can be found in Table 2.

4. DISCUSSION

The high-resolution data from the *ROSAT* detectors reveal that the morphology of the PSR B1823−13 system is very similar to other young neutron stars such as the Crab pulsar, the Vela pulsar, PSR B1509−58, and PSR B1951+32. The common morphology shared by these young neutron stars finds the pointlike component, presumably the neutron star, embedded in a compact nebular component which, it is speculated, defines the boundary where the ram pressure of the relativistic particle wind from the rapidly rotating neutron star achieves equilibrium with the pressure of an associated SNR (Rees & Gunn 1974). The model of Rees & Gunn (1974) was developed in response to the observation of an X-ray emitting torus surrounding the Crab pulsar (Brinkmann, Aschenbach, & Langmeier 1985) which has a physical size of $\approx$0.1 pc for an assumed distance of 2 kpc to the Crab Nebula; about 25% of the size of the compact nebula observed in PSR B1823−13. It is interesting to compare the linear scale size of the PSR B1823−13 compact nebula with those of the other young neutron stars. Our derived linear scale size of $r_{CN} \approx 19''$ implies a physical dimension of $\approx$0.37 pc assuming a distance of 4 kpc. The Vela pulsar compact nebula has a linear scale size of $\sim 1'$ which corresponds to a physical dimension of $\approx$0.15 pc assuming a distance of 500 pc (Harnden et al. 1985; Ögelman & Zimmermann 1989) which is almost a factor of 3 less than observed in PSR B1823−13. The compact nebula of PSR B1951+32 is observed to have a linear scale size of $\sim 1'$ which, at an assumed distance of 2.5 kpc corresponds to a physical dimension of $\approx$0.70 pc, or about a factor of 2 larger than is observed in PSR B1823−13 (Safi-Harb et al. 1995). The very young pulsar PSR B1509−58, associated with the SNR MSH 15−52, has recently been revealed to be embedded in a compact nebula of scale size $\sim 50''$ corresponding to a physical dimension of $\approx$0.9 pc at an assumed distance of 4.2 kpc (Greiveldinger et al. 1995); about a factor of 2.5 times the size observed in PSR B1823−13. In short, the scales of the observed compact nebulae surrounding young neutron stars are quite disparate, spanning a factor of about 9 in physical size. We note there that all the compact nebulae observed surrounding young neutron stars are in systems in which a supernova remnant association is established. In the model of Rees & Gunn (1974) the physical size of the compact nebula is related to the size of the SNR in which

TABLE 2

90% CL Upper Limits on the Parameters[a] of the PSR B1823−13 System

Parameter	Value	F_x (10^{-12} ergs cm^{-2} s^{-1})	L_x (10^{33} ergs s^{-1})
Point Source			
Blackbody ($R = 8$ km, $D = 4$ kpc)	$kT_\infty \leq 0.21$ keV	≤6	≤16
Power law ($\alpha = -1.0$, $D = 4$ kpc)	...	≤2.2	≤3.8
Compact Nebula			
Power law ($\alpha = -2.0$, $D = 4$ kpc)	...	≤2.4	≤4.0
Extended Component			
Raymond-Smith ($T = 10^7$ K, solar abundance)	...	≤10	
Power law ($\alpha = -1.0$, $D = 4$ kpc)	...	≤5.0	≤8.3

[a] To derive the upper limits the N_H was held fixed at 4×10^{22} cm^{-2}. In the case of the blackbody model the luminosity is the bolometric luminosity which for the others it is the luminosity in the 0.5–2.4 keV band.

the system is embedded under the assumption that the remnant is a spherical cavity and has had a uniform particle flux injected into its volume over the entire remnant lifetime. The observed radius of the PSR B1823−13 compact nebula of ≈20″ implies that the radius of the supernova remnant cavity with which the system is interacting, according to the Rees & Gunn (1974) prescription, should be on the order of about 2′–2.′5; not unlike the size of the extended component we observe surrounding the PSR B1823−13 system. This statement is couched with the caveat that the Rees & Gunn (1974) model, while successful in predicting the size of the Crab and PSR B1509−58 compact nebulae, is inadequate when applied to the Vela and PSR B1951+32 compact nebulae and SNRs. The discrepancies, however, may be due to the presence of a jet which carries away a significant fraction of the particle energy in the case of the Vela pulsar system (Markwardt & Ögelman 1995) while in the PSR B1951+32 system the fact that the pulsar/compact nebula has "broken out" of its SNR shell (Safi-Harb et al. 1995) may invalidate the Rees & Gunn (1974) model. The value of $L_X/\dot{E}$ of ≤0.15% indicates that, as in the other young neutron star/compact nebula systems, the bulk of the particle and field energy originating near the neutron star stellar surface is largely unconfined within the compact nebula and must be deposited elsewhere (e.g., within the SNR or ISM).

The similarity of the Rees & Gunn (1974) prediction for the size of the supernova cavity and the observed size of the extended component (see Fig. 1) surrounding PSR B1823−13 lead us to entertain the notion that we are imaging the hot interior of the SNR associated with the neutron star. Previous searches in the radio band at 1465 MHz, 1665 MHz, and 4835/4885 MHz using the VLA D and C/D configurations by Braun et al. (1989) failed to detect any evidence for the putative SNR associated with PSR B1823−13 on a scale of ∼10′ radius. The extended component observed in the X-ray image (see Fig. 1) would have been below the surface brightness detection limit of the Braun et al. (1989) survey and the ∼45″ resolution of their survey would have failed to resolve the compact nubular component as well. Therefore, our interpretation of the extended component as the remnant of the supernova of the progenitor of PSR B1823−13 is not in conflict with extant radio data. The very high plasma temperature implied by the modeling is consistent with the large extinction toward PSR B1823−13 which would result in the cooler edges of the remnant being absorbed out and therefore unobservable in our X-ray image. Follow-up observations in the radio band sensitive to radial scale sizes of ∼2′–3′ may provide confirmation of the presence of the SNR associated with PSR B1823−13.

The morphology of the extended component in Figure 1 also leads to an alternate interpretation for the origin of this emission feature. The extension along the north-east–south-west direction at a position angle of ∼30° (we define position angle as 0° to the north, 90° to the east) is reminiscent of the cometary morphology of the pulsar wind nebulae (PWNs) observed around other neutron star systems such as PSR B1957+20 (Kulkarni & Hester 1988) and PSR B2224+65 (Cordes, Romani & Lundgren 1993) which is associated with the Guitar nebula. The formation of a PWN is the result of the balance between the pressure of the energetic neutron star wind ($\dot{E}/4\pi R^2 c$) and the ram pressure of the ambient interstellar medium ($\rho_0 v_p^2$) where $\dot{E}$ is the spin-down energy of the neutron star, R is the physical distance from the neutron star to the apex of the cometary feature, ρ_0 is the mass density of the interstellar medium, and v_p is the velocity of the neutron star with respect to the interstellar medium. From our Figure 1 we observe a scale size for the PWN of ∼40″ implying a physical size, assuming a 4 kpc source distance, of ∼0.8 pc. The absence of SNRs associated with some young neutron stars has led to the conjecture that the neutron star progenitors exploded in low-density environments where the mean ambient ISM is of the order $n_0 \sim 0.01$ cm^{-3} (Bhattacharya 1990). This conjecture leads to a natural explanation for the lack of a detectable SNR associated with young neutron stars due to the rapid expansion and dissipation of the remnant and a resultant observable lifetime of ≤10,000 yr. Adopting this value of n_0 and with our measured physical scale size the implied pulsar velocity relative to the ambient ISM is $v_p \sim$ 90 km s^{-1}; not atypical for an average neutron star based upon proper motion studies where $\langle v_{\rm PSR} \rangle \cong 200$ km s^{-1} (Harrison, Lyne, & Anderson 1993). However, recent work by Frail et al. (1994a) based upon a study of young neutron stars with assured or firm SNR associations lead to an average ambient ISM into which the SNR is expanding of $n_0 \sim 0.2$ cm^{-3} and implies a much lower pulsar velocity of $v_p \sim 20$ km s^{-1}. The same authors also derive a mean pulsar velocity based on their sample of $v_p \sim 480$ km s^{-1} (Frail et al. 1994a) which is consistent with the value of (450 ± 90) km s^{-1} derived by Lyne & Lorimer (1994) after a reevaluation of the proper motion studies which takes into account selection effects and the new Galactic distance model of Taylor & Cordes (1993). If we adopt a pulsar velocity of 450 km s^{-1} the inferred ISM ambient density into which the pulsar is moving attains the seemingly unlikely value of $n_0 \sim 0.0004$ cm^{-3}. Given the improbability of such a rarefied ISM we conclude that if the extended emission feature is correctly interpreted as a PWN then PSR B1823−13 is not a "high-velocity" neutron star (i.e., has a velocity through the ISM significantly less than the currently accepted mean of 450 km s^{-1}) but rather has a transverse velocity of $v_p \leq 100$ km s^{-1}. This limit places PSR B1823−13 not more than about 1.′7 from its birth place and moving to the north-east at a position angle ∼30° (position angle 0° to the north, 90° to the east). Of course, we cannot rule out the possibility that the ISM ambient density surrounding the PSR B1823−13 system is exceedingly small and, in fact, this was a conclusion of Braun et al. (1989) used to explain their lack of a SNR detection. Distinguishing the two possibilities will necessarily have to be the providence of subsequent investigation.

The modeling of the point source component can be interpreted in terms of a broad range of models for the cooling of neutron stars (for a recent review see Ögelman 1994). Assuming an interstellar neutral hydrogen column density of 4×10^{22} cm^{-2} our derived conservative upper limit for the surface temperature of $kT_\infty \leq 0.21$ keV for an 8 km neutron star at a distance of 4 kpc lies well above the range of models incorporating both standard and exotic scenarios and is plotted, along with some cooling curves for an observer at infinity taken from the literature, in Figure 4. On the other hand, if the appropriate neutron star radius is taken as 16 km (i.e., hard equation of state) then the upper limit is reduced to $kT_\infty \leq 0.11$ keV which, while not inconsistent with the standard models, begins to challenge the currently adopted cooling scenarios (see Fig. 4). Lower

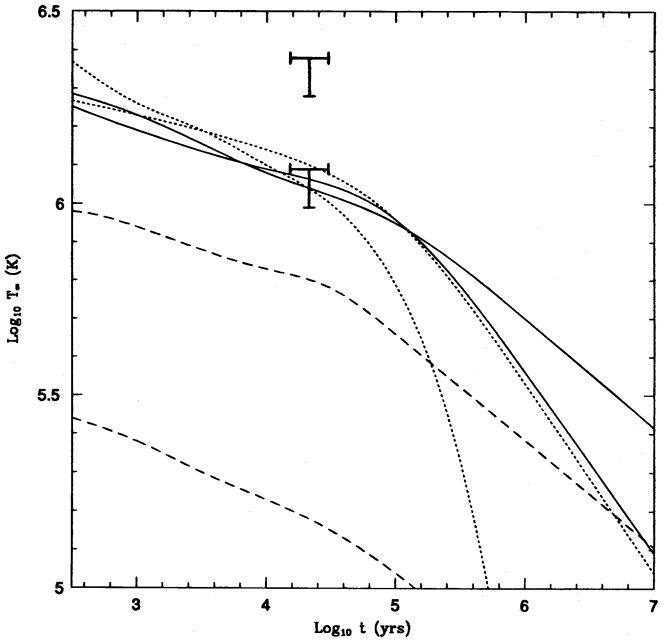

FIG. 4.—The upper limits of the surface temperature of PSR B1823−13 from the bare neutron star for an observer at infinity compared with some representative cooling curves taken from the literature. The higher point is for an 8 km radius neutron star at a distance of 4 kpc while the lower point is for a 16 km radius neutron star at a distance of 4 kpc. Both limits were derived assuming an intersellar equivalent neutral hydrogen column density of 4×10^{22} cm^{-2}. The short-dashed and solid curves are standard cooling with and without superfluids while the long-dashed curves are for some representative exotic cooling models (pion condensate for the upper curve and direct URCA for the lower curve). A review of standard and nonstandard cooling can be found in Finley (1994) and Ögelman (1994).

values of the interstellar column density serve to reduce the inferred limits and call the standard scenarios even more into question. *We note that the best-fitting value for the point source contribution inferred from the HRI data yields an upper limit on the surface temperature for all reasonable ranges of the parameters which falls well below the standard cooling curves and would imply the presence of some exotic cooling agents such as pion condensates or direct URCA cooling.* The interpretation of the point source emission as arising solely as a result of cooling from the neutron star surface is, however, fraught with difficulty. Observations of the Vela pulsar, for example, reveal that the soft emission which is interpreted as arising from cooling originates from an area which is much smaller than the canonical neutron star surface area (Ögelman et al. 1993) while observations of older neutron stars ($\tau \approx 10^5$ yr) reveal the presence of a high-energy tail of an unknown origin (see Finley 1994 and references therein). Another possibility is that the point source emission arises in the magnetosphere of the rapidly rotating neutron star and is a result of nonthermal processes. Ögelman (1994) found an empirical law based on a large sample of X-ray emitting neutron stars which predicts the luminosity based on the spin parameters of the neutron star in question which agrees well with the observations, $L_X \cong 1.3 \times 10^{-10} (B\Omega^2)^{2.7}$ ergs s^{-1}. All of the known or suspected magnetospheric emitters (such as the Crab, the LMC pulsar, etc.) agree well with this empirical law while the cooling candidates (such as PSR B0656+14, PSR B1055−52, and Geminga) show large deviations from the general trend and, it is argued, supports the interpretation that they are indeed cooling (Ögelman 1994). Application of the empirical law to PSR B1823−13 ($B = 2.8 \times 10^{12}$ G, $\Omega = 62.2$ rad s^{-1}) predicts an X-ray luminosity of $L_X = 2.6 \times 10^{33}$ ergs s^{-1} which can be compared with our limit for a Crab-like spectrum of $L_X \leq 3.8 \times 10^{33}$ ergs s^{-1}. Our limit is only marginally larger than that predicted by the empirical model and may indicate that we are seeing nonthermal photons from an electromagnetic process in the outer magnetosphere or photons originating in a hard tail like that observed in the older neutron stars.

5. SUMMARY

The *ROSAT* PSPC and HRI data presented here reveal that the young neutron star PSR B1823−13 possesses a morphology not unlike other young neutron stars of a similar age. The point source component, presumably the neutron star, is embedded in a compact nebula of radius $\sim 20''$ and the point source plus compact nebula is surrounded by an extended diffuse emission region of size $\sim 4'$. The size of the extended component is consistent with that expected for the SNR associated with a compact nebula of the observed size according to the model of Rees & Gunn (1974) and lead us to speculate that we are seeing the hot interior of the supernova cavity in which PSR B1823−13 was born. Alternatively, the extended component may be interpreted as a PWN where the spin-down powered wind of the rapidly rotating neutron star comes into pressure equilibrium with the ambient ISM. In that case the data imply that either (a) PSR B1823−13 is not a high-velocity neutron star but has a transverse velocity of ≤ 100 km s^{-1} significantly below the currently accepted mean of 450 km s^{-1} or (b) the ambient interstellar medium in which PSR B1823−13 is found is extremely rarefied, an interpretation previously used to explain the absence of any detectable SNR. The low-velocity neutron star scenario implies that PSR B1823−13 has not moved more than 1.′7 from its birth position and currently has a proper motion to the northeast at a position angle of $\sim 30°$. The compact nebula surrounding PSR B1823−13 shares characteristics of the other young neutron stars with a similar morphology in that (a) its physical size is consistent with the size of the extended component in which it is found, and (b) its luminosity is only a small fraction of the spin-down energy available from the rapidly rotating neutron star and thus is largely transparent to the bulk of the emergent radiation. Conservative limits derived for the point source emission do not challenge standard cooling scenarios for neutron stars unless one allows a relaxation of stringent bounds on the neutron stars parameters or the intervening neutral hydrogen column density. A comparison of the derived luminosity limits with the prediction of an empirical luminosity law suggests that the point source emission may arise as a result of electromagnetic processes in the outer magnetosphere. Subsequent observations at high spatial resolution in the X-ray, radio, and infrared should sort out some of the issues raised by the observations presented here.

The authors would like to thank D. Frail and N. Kassim for helpful discussions concerning radio measurements of compact systems and B. Savage for guidance on issues related to the O6 star HD 169727. We are indebted to J. Gaidos for a critical reading of the manuscript and the referee J. Cordes for a thoughtful review. This research was supported in part by NASA grant NAG 5-2492 and a grant from the Purdue Research Foundation.

REFERENCES

Bhattacharya, D. 1990, J. Astrophys. Astron., 11, 125
Bohlin, R. C., Savage, B. D., & Drake, J. F. 1976, ApJ, 224, 132
Braun, R., Goss, W. M., & Lyne, A. G. 1989, ApJ, 340, 355
Brinkmann, W., Aschenbach, B., & Langmeier, A. 1985, Nature, 313, 662
Caraveo, P. A. 1993, ApJ, 415, L111
Clifton, T. R., & Lyne, A. G. 1986, Nature, 320, 43
Clifton, T. R., Lyne, A. G., Jones, A. W., McKenna, J., & Ashworth, M. 1992, MNRAS, 254, 177
Cordes, J. M. 1986, ApJ, 311, 183
Cordes, J. M., Romani, R. W., & Lundgren, S. C. 1993, Nature, 362, 133
Finley, J. P. 1994, in AIP Conf. Proc., No 313, The Soft X-Ray Cosmos, ed. E. Schlegel & R. Petre (New York: AIP), 68
Finley, J. P., & Ögelman, H. 1993, IAU Circ., No. 5787
Finley, J. P., & Ögelman, H. 1994, ApJ, 434, L25
Frail, D. A., Goss, W. M., & Whiteoak, J. B. Z. 1994a, ApJ, 437, 781
Frail, D. A., Kassim, N. E., & Weiler, K. W. 1994b, AJ, 107, 1119
Garmany, C. D., & Vacca, W. D. 1991, PASP, 103, 347
Greiveldinger, C., Caucino, S., Massaglia, S., Ögelman, H., & Trussoni, E. 1995, ApJ, 454, 855
Gunn, J. E., & Ostriker, J. P. 1970, ApJ, 160, 979
Harnden, F. R., Jr., Grant, P. D., Seward, F. D., & Kahn, S. M. 1985, ApJ, 299, 828
Harrison, P. A., Lyne, A. G., & Anderson, B. 1993, MNRAS, 261, 113
Johnston, S., Lyne, A. G., Manchester, R. N., Kniffen, D. A., D'Amico, N., Lim, J., & Ashworth, M. 1992, MNRAS, 255, 401
Kassim, N. E., & Weiler, K. W. 1990, Nature, 343, 146
Kifune, T., et al. 1995, ApJ, 438, 91
Kulkarni, S. R., & Hester, J. J. 1988, Nature, 335, 801
Lampton, M., Margon, B., & Bowyer, S. 1976, ApJ, 208, 117
Lyne, A. G., & Lorimer, D. R. 1994, Nature, 369, 127
Markwardt, C., & Ögelman, H. 1995, Nature, 375, 40
Odegard, N, 1986, AJ, 92, 1372
Ögelman, H. 1994, Wisconsin Astrophysics, preprint 513
Ögelman, H., Finley, J. P., & Zimmermann, U. 1993, Nature, 361, 136
Ögelman, H., & Zimmermann, H.-U. 1989, A&A, 214, 179
Pfeffermann, E., et al. 1986, Proc. SPIE, 733, 519
Rees, M. J., & Gunn, J. E. 1974, MNRAS, 167, 1
Safi-Harb, S., Ögelman, H., & Finley, J. P. 1995, ApJ, 439, 722
Shull, J. M., Fesen, R. A., & Saken, J. M. 1989, ApJ, 346, 860
Taylor, J. H., & Cordes, J. M. 1993, ApJ, 411, 674
Taylor, J. H., Manchester, R. N., & Lyne, A. G. 1993, ApJS, 88, 529
———. 1995, Catalog of Pulsars, private communication
Thompson, D. J., et al. 1994, ApJ, 436, 229
Vacanti, G., et al. 1991, ApJ, 377, 467